Fires increase Amazon forest productivity through increases in diffuse radiation

A. Rap, D. V. Spracklen, L. Mercado, C. L. Reddington, J. M. Haywood, R. J. Ellis, O. L. Phillips, P. Artaxo, Damien Bonal, Natalia Restrepo-Coupe, et al.

AGU PUBLICATIONS

Geophysical Research Letters

RESEARCH LETTER
10.1002/2015GL063719

Key Points:
- First estimate of diffuse radiation fertilization due to Amazon BBA
- This effect offsets 33–65% of the annual regional carbon emissions from BBA
- Counteracts some of the observed effect of drought on tropical production

Supporting Information:
- Figures S1–S6

Correspondence to:
A. Rap,
a.rap@leeds.ac.uk

Citation:
Rap, A., et al. (2015), Fires increase Amazon forest productivity through increases in diffuse radiation, *Geophys. Res. Lett.*, *42*, 4654–4662, doi:10.1002/2015GL063719.

Received 3 MAR 2015
Accepted 19 MAY 2015
Accepted article online 25 MAY 2015
Published online 9 JUN 2015

Fires increase Amazon forest productivity through increases in diffuse radiation

A. Rap[1], D. V. Spracklen[1], L. Mercado[2,3], C. L. Reddington[1], J. M. Haywood[4], R. J. Ellis[3], O. L. Phillips[5], P. Artaxo[6], D. Bonal[7], N. Restrepo Coupe[8], and N. Butt[9]

[1]School of Earth and Environment, University of Leeds, Leeds, UK, [2]College of Life and Environmental Sciences, University of Exeter, Exeter, UK, [3]Centre for Ecology and Hydrology, Wallingford, UK, [4]College of Engineering Mathematics and Physical Science, University of Exeter, Exeter, UK, [5]School of Geography, University of Leeds, Leeds, UK, [6]Institute of Physics, University of São Paulo, São Paulo, Brazil, [7]INRA UMR Ecologie et Ecophysiologie Forestières, Champenoux, France, [8]Plant Functional Biology & Climate Change Cluster, University of Technology Sydney, Ultimo, New South Wales, Australia, [9]School of Biological Sciences, University of Queensland, St. Lucia, Queensland, Australia

Abstract Atmospheric aerosol scatters solar radiation increasing the fraction of diffuse radiation and the efficiency of photosynthesis. We quantify the impacts of biomass burning aerosol (BBA) on diffuse radiation and plant photosynthesis across Amazonia during 1998–2007. Evaluation against observed aerosol optical depth allows us to provide lower and upper BBA emissions estimates. BBA increases Amazon basin annual mean diffuse radiation by 3.4–6.8% and net primary production (NPP) by 1.4–2.8%, with quoted ranges driven by uncertainty in BBA emissions. The enhancement of Amazon basin NPP by 78–156 Tg C a^{-1} is equivalent to 33–65% of the annual regional carbon emissions from biomass burning. This NPP increase occurs during the dry season and acts to counteract some of the observed effect of drought on tropical production. We estimate that 30–60 Tg C a^{-1} of this NPP enhancement is within woody tissue, accounting for 8–16% of the observed carbon sink across mature Amazonian forests.

1. Introduction

An increase in carbon storage has been observed in undisturbed forests across Amazonia during the last few decades [*Phillips et al.,* 2009]. Several mechanisms have been suggested as possible causes of this carbon sink, including changes in temperature, carbon dioxide, precipitation, clouds, and solar radiation [*Nemani et al.,* 2003; *Lewis et al.,* 2004; *Davidson et al.,* 2012]. Here we explore the impact of biomass burning aerosol (BBA) on diffuse radiation and Amazon forest productivity.

The efficiency of plant photosynthesis increases under diffuse sunlight, a phenomenon that has been explained theoretically [*Roderick et al.,* 2001] and widely observed [*Gu et al.,* 2003; *Niyogi et al.,* 2004; *Oliveira et al.,* 2007; *Doughty et al.,* 2010]. Leaf photosynthesis increases nonlinearly with solar radiation, becoming saturated at light levels that can be exceeded on bright days [*Gu et al.,* 2003; *Mercado et al.,* 2009]. Under clear-sky conditions, sunlight is mainly direct, resulting in sunlit leaves being light saturated, whereas shaded leaves receive little sunlight. In the presence of optically thin clouds or atmospheric aerosol, direct radiation incident on the plant canopy is reduced due to sunlight scattering, while diffuse radiation is increased. The reduction in direct solar radiation has an inhibiting effect on photosynthesis, while the increase in diffuse radiation illuminates parts of the canopy that would otherwise be shaded, increasing photosynthesis. The net effect on photosynthesis is determined by the balance of these two competing effects, and it is in tropical regions such as the Amazon basin where this balance leads to the largest positive effect: while canopy carbon assimilation is often greatly reduced around midday as leaves shut down stomata (due to bright, hot, and high vapor pressure deficit conditions), diffuse light acts to reduce this depression. However, if clouds and aerosols are optically thick, then both direct and diffuse radiation incident on the plant canopy are reduced, resulting in a decrease in photosynthesis.

Previous work has shown that increased diffuse radiation due to anthropogenic aerosols has led to a 25% increase in the global land-carbon sink in recent decades [*Mercado et al.,* 2009]. Across the Amazon, emissions from fossil fuel combustion are limited and the wet season atmosphere is relatively pristine, being dominated by emissions of aerosols produced by the vegetation itself [*Martin et al.,* 2010]. In contrast, during the dry season, numerous fires [*Aragão et al.,* 2008] emit large quantities of carbonaceous aerosol into the

atmosphere, increasing aerosol concentrations across the Amazon basin [*Martin et al.,* 2010; *Andreae et al.,* 2012], altering surface radiation [*Schafer et al.,* 2002], and potentially plant productivity. Observations of smoke increasing Amazon forest productivity through changes to radiation have been recorded [*Oliveira et al.,* 2007; *Doughty et al.,* 2010; *Artaxo et al.,* 2013], but the impact of regional smoke pollution on diffuse radiation and Amazon vegetation has not yet been explored. Here we quantify the impact of biomass burning on atmospheric aerosol, solar radiation, and plant productivity of the Amazon basin biosphere.

2. Methodology

We simulate atmospheric aerosol concentrations using a global aerosol model [*Mann et al.,* 2010] combined with satellite-derived biomass burning aerosol (BBA) emissions [*van der Werf et al.,* 2010]. The impact of changing aerosol on surface radiation is quantified using a radiative transfer model [*Rap et al.,* 2013]. Finally, plant photosynthesis is simulated using a land surface model [*Mercado et al.,* 2009].

2.1. Aerosol Model

We simulated aerosol using the 3-D GLObal Model of Aerosol Processes (GLOMAP) [*Mann et al.,* 2010]. The aerosol size distribution is simulated using a two-moment modal scheme. The model includes a description of nucleation, coagulation, condensation of gas phase species, in-cloud and below-cloud aerosol scavenging and deposition, dry deposition, and cloud processing. The aerosol species included in GLOMAP are black carbon (BC), particulate organic matter (POM), sulfate, sea salt, and dust. The model is driven by analyzed meteorology from the European Centre for Medium Range Weather Forecasts (ECMWF), updated every 6 h and linearly interpolated onto the model time step (30 min). Using analyzed meteorology allows us to isolate the impact of BBA on diffuse radiation from the highly uncertain impacts of aerosol on atmospheric circulation and rainfall [*Andreae et al.,* 2004; *Tosca et al.,* 2013]. The horizontal resolution of the model is $2.8° \times 2.8°$, with 31 vertical model levels between the surface and 10 hPa. Yearly varying, monthly mean fire emissions of SO_2, BC, and POM were taken from the Global Fire Emissions Database (GFED3) [*van der Werf et al.,* 2010]. The GFED3 emissions are derived using estimates of burnt area, active fire detections, and plant productivity from the Moderate Resolution Imaging Spectroradiometer (MODIS) instrument, combined with estimates of fuel loads and combustion completeness for each monthly time step from the Carnegie-Ames-Stanford-Approach (CASA) biogeochemical model [*van der Werf et al.,* 2010]. The injection heights of the fire emissions were distributed in GLOMAP between the surface and 6 km [*Dentener et al.,* 2006].

2.2. Radiative Transfer Model

The aerosol effect on direct and diffuse radiation was calculated using a radiative transfer model [*Edwards and Slingo*, 1996; *Rap et al.,* 2013] with six bands in the short-wave and nine bands in the long-wave, based on the two-stream equations at all wavelengths. Aerosol scattering and absorption coefficients together with asymmetry parameters are calculated for each aerosol size mode and spectral band, as described in *Bellouin et al.* [2013]. We used a monthly mean climatology for water vapor, temperature, and ozone based on ECMWF reanalysis data, together with surface albedo and cloud optical depth fields from the International Satellite Cloud Climatology Project (ISCCP-D2) [*Rossow and Schiffer*, 1999]. The diffuse radiation flux was obtained by subtracting the direct flux (calculated using an Eddington two-stream scattering solver) from the total flux (calculated using a delta-Eddington solver).

2.3. Land Surface Model

The Joint UK Land Environment Simulator (JULES) land surface model represents the fluxes of water, energy, and carbon between the land and the atmosphere [*Best et al.,* 2011; *Clark et al.,* 2011]. This study employs the canopy radiation-photosynthesis scheme in JULES that accounts for effects of diffuse radiation on sunlit and shaded photosynthesis [*Mercado et al.,* 2007, 2009], using a multilayer canopy model with 10 layers. The model estimates radiation interception and photosynthesis at each layer, by splitting leaves into sunlit and shaded categories depending on sunlit fraction. Sunlit leaves receive both direct and diffuse radiation, and shaded leaves only receive diffuse radiation. The standard photosynthesis equations described by *Clark et al.* [2011] are used, while leaf area index (LAI) is prescribed for each plant functional type based on the MODIS LAI product. The radiation model is the two-stream model from *Sellers* [1985] with a modification to include sunfleck penetration [*Dai et al.,* 2004; *Mercado et al.,* 2007, 2009]. The model is run with a spatial resolution of 0.5° across the domain and forced with meteorological driving data

with a temporal resolution of 3 h. The meteorological components consist of 2 m air temperature and specific humidity, precipitation, 10 m wind speed, and surface pressure. The data were derived using the methodology for bias correction [*Weedon et al.,* 2011] of the ECMWF ERA-Interim reanalysis product. The model uses downward direct and diffuse short-wave and long-wave radiation derived from our radiative transfer model. The soil hydrology utilized the van Genuchten relationships [*van Genuchten*, 1980] and parameters derived from the *Harmonized World Soil Database* [2012].

2.4. Model Simulations

We performed five simulations for the period January 1998 to December 2007: (i) all BBA emissions included (the control simulation), (ii) deforestation fires (as classified by the fire emissions inventory [*van der Werf et al.,* 2010]) switched off, (iii) all fires switched off, (iv) BBA emissions scaled by a factor of 3 (3 × BBA), and (v) BBA emissions scaled by a factor of 6 (6 × BBA). These simulations account for uncertainty in the magnitude of BBA emissions, with previous studies [*Kaiser et al.,* 2012; *Tosca et al.,* 2013] increasing emissions by up to a factor of 6 to match observed aerosol optical depth (AOD).

2.5. Observations Used in Model Evaluation

The simulated concentrations of particles less than 2.5 μm diameter (PM2.5), AOD, total and diffuse radiation, and gross primary productivity (GPP) were evaluated using observations across the Amazon. The PM2.5 measurements were made using gravimetric filter analysis at two ground stations in Brazil: Balbina (1.917°S, 59.487°W; October 1998 to May 2003), a remote forest site in central Amazonia, and Porto Velho (8.687°S, 63.866°W; September 2009 to December 2011), a heavily biomass burning impacted site in southwestern Amazonia. Measurements of AOD at 500 nm were made using Sun-sky scanning spectral radiometers at four stations in the Aerosol Robotic Network (AERONET): Rio Branco, Alta Floresta, and Cuiabá-Miranda in Brazil and Santa Cruz in Bolivia. These sites are strongly influenced by biomass burning emissions in the dry season [*Hoelzemann et al.,* 2009]. We used Level 2 data available between 1998 and 2008, with all years of data available at Alta Floresta and Santa Cruz, ~7 years at Cuiabá-Miranda, and ~8 years at Rio Branco. At Caxiuana, Brazil (1.738°S, 51.453°W), total and diffuse radiation observations [*Butt et al.,* 2010] have been collected every 2 min between March 2005 and August 2006, using a BF3 sunshine sensor [*Wood et al.,* 2003] (Delta-T Devices, Cambridge, UK), located at a height of 50 m, about 20 m above the top of the forest canopy. At Tapajos, Brazil (2.857°S, 54.959°W), total and diffuse radiation were measured using a BF3 sunshine sensor (2004–2006), and C fluxes were measured using a close-path eddy covariance (EC) system [*Saleska et al.,* 2003; *Restrepo-Coupe et al.,* 2013]. The high-frequency flux data were averaged to hourly values for the January 2002 to January 2006 period. The EC sensor is placed at a height of 63 m over a height of 35–40 m evergreen forest canopy. At Guyaflux, French Guiana (5.280°N, 52.926°W), total and diffuse radiation were measured using a BF3 sunshine sensor and GPP data calculated using eddy flux data [*Bonal et al.,* 2008] collected every 30 min between January 2007 and December 2009, at a height of 57 m (approximately 22 m above the canopy height) from an undisturbed mature evergreen broadleaf tropical wet ecosystem (for the GPP observations, only measurements between 9 A.M. and 5 P.M. local time were used).

To estimate the contribution of increased diffuse radiation to the observed carbon sink, we compared against the RAINFOR network of forest inventory plots across the Amazon basin [*Phillips et al.,* 2009]. This network indicates that in the decades before 2007, mature forests across the Amazon basin have been accumulating carbon in wood at an estimated rate of 0.37 Pg C a^{-1}. To partition our calculated change in net primary productivity (NPP) to woody NPP, we used a global data set of ecosystem NPP allocation in tropical forests [*Malhi et al.,* 2011] that suggests a 39 ± 10% partitioning into wood.

3. Results and Discussion

Figure 1 shows simulated AOD, radiation, and GPP compared to observations from several sites across the Amazon basin. As in previous studies [*Kaiser et al.,* 2012; *Tosca et al.,* 2013], when using standard BBA emissions, simulated AOD underestimates the observed values (normalized mean bias (NMB) = −41%). With BBA emissions scaled by a factor of 3, the model typically overestimates AOD (NMB = 19%), while the correlation coefficient between the modeled and the observed values remains high ($r = 0.89$ for both cases). We therefore use these two simulations as a rough lower and upper bound estimate of BBA emissions. As we show later, this uncertainty in emissions results in a factor of ~2 uncertainty on the impact of BBA on forest

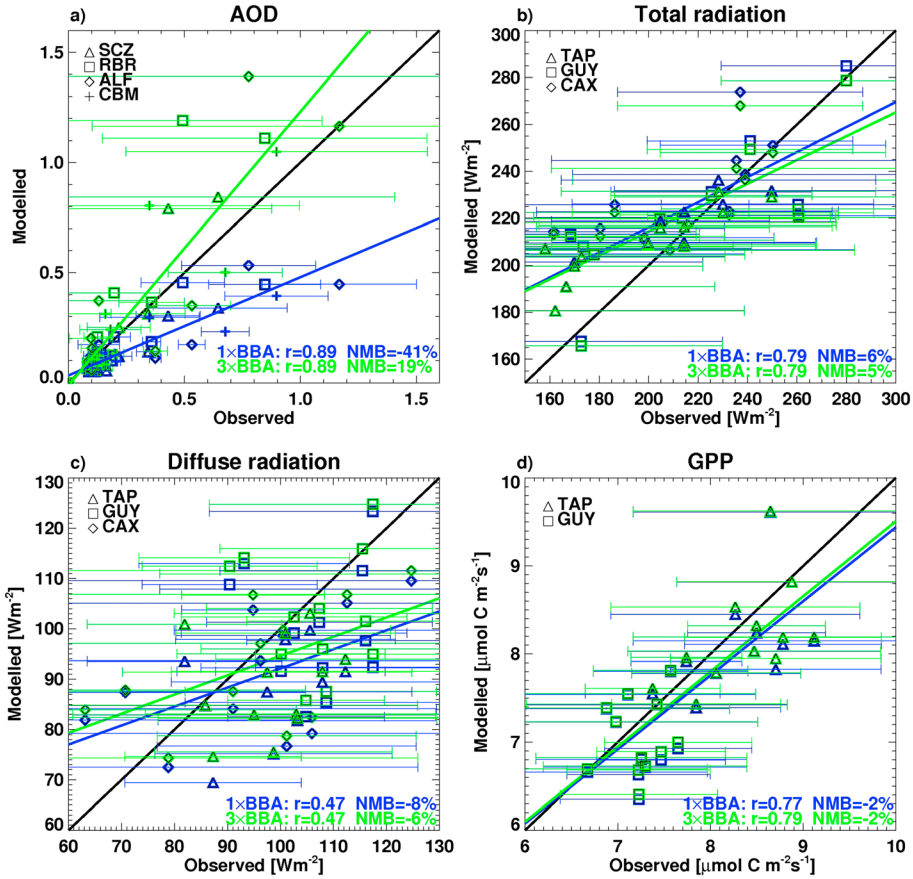

Figure 1. Scatterplot of monthly mean observed (with error bars showing 1 standard deviation in daily mean) against 1 × BBA modeled (blue) and 3 × BBA modeled (green) (a) AOD, (b) short-wave total radiation, (c) short-wave diffuse radiation, and (d) GPP at various Amazonian sites (locations shown in Figure 3a). The Guyaflux GPP values were calculated from values corresponding to 9 A.M. to 5 P.M. local time only, assuming zero GPP between 5 P.M. and 9 A.M. Lines of best fit between modeled and observed values for all sites, together with correlation coefficients (*r*) and normalized mean biases (NMB), are included in each panel.

carbon uptake. Simulated radiation and GPP compare reasonably well against observations (NMB < 10%). The model also simulates the observed seasonal cycle with PM2.5, AOD, and total radiation peaking during the dry season, while GPP peaks during the wet season (Figure S1 in the supporting information). Compared to AOD, radiation and GPP are less sensitive to increasing BBA emissions, due to their larger sensitivity to other factors such as clouds. However, the model is able to simulate the reduction in total radiation and the increases in diffuse radiation and GPP (Figures 1b–1d) when BBA emissions are increased.

Figure 2 shows the simulated and observed response of GPP to photosynthetically active radiation (PAR), under both direct and diffuse radiation conditions. Observed and simulated GPP increase with increased PAR, saturating at high PAR. Also, for the same amount of PAR, both observed and simulated GPP are increased by ~45% under diffuse compared to direct light conditions. The comparison demonstrates that the model is capable of simulating the observed increase in photosynthesis in tropical forests of the Amazon basin under diffuse sunlight.

Figure 3 shows the simulated effect of biomass burning on PM2.5, diffuse radiation, GPP, and NPP in the Amazon region. Biomass burning has the greatest impact during the Amazon basin dry season (considered here as June to November), with little impact during the wet season (December to May). This is due to the seasonal cycle of Amazonian fires which peak in the dry season [*van der Werf et al.,* 2010], combined with an opposing seasonal cycle in cloud fraction. The large cloud fraction over the Amazon basin during the wet season dominates diffuse radiation, masking any aerosol-driven changes in radiation. Biomass burning typically has the largest impact in August, when fire emissions are strong and cloud cover is minimal [*Holben et al.,* 2001].

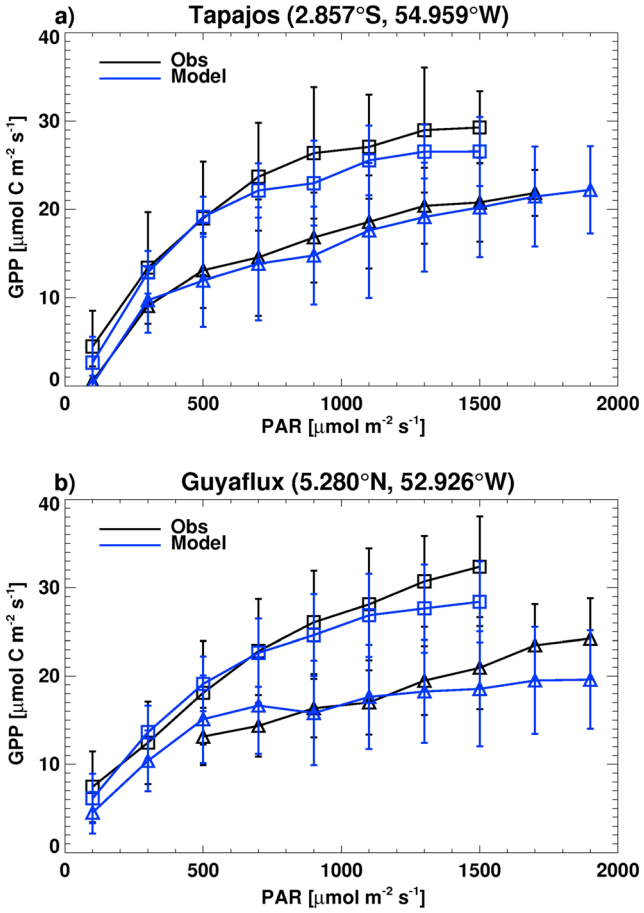

Figure 2. Observed (black) and modeled (blue) light response of GPP to direct (triangles) and diffuse (squares) photosynthetically active radiation (PAR) averaged over bins of 200 μmol quanta m^{-2} s^{-1} at (a) Tapajos (2002–2005) and (b) Guyaflux (2006–2007). Error bars show 1 standard deviation of all values. Data points are split into "diffuse" and "direct" conditions using diffuse fractions > 80% and < 25% to discriminate between these two cases.

We calculate that BBA increases Amazon basin (defined as the 6×10^6 km^2 area shown by the black boundary in Figure 3) annual mean PM2.5 (48–145%), diffuse radiation (3.4–6.8%), GPP (0.7–1.6%), and NPP (1.4–2.8%), with the quoted ranges driven by a factor of 3 uncertainty in BBA emissions. In August, impacts are larger with simulated increases in Amazon basin mean GPP of 2.8–5.1% and NPP of 5.4–8.8% (Figures 3 and S2). For comparison, we calculated the fertilization effect caused by the increase in atmospheric CO_2 by comparing two 10 year simulations, one using 2007 and the other 1998 CO_2 concentrations. We found a 0.3% increase in annual GPP (i.e., 3% over the 10 year period) due to CO_2 fertilization in the Amazon basin during 1998–2007. This is consistent with the 0.25 ± 0.1% multimodel mean annual increase in GPP for tropical South America calculated using the nine Dynamic Global Vegetation Models (DGVMs) from *Sitch et al.* [2015]. This suggests that the diffuse radiation fertilization effect due to BBA over the Amazon during 1998–2007 was larger than the CO_2 fertilization effect that occurred over this period.

A large fraction of fire across Amazonia is caused by human activity, with fire used to clear forested land for agriculture [*Aragão et al.,* 2008]. We simulated the impact of these Amazon deforestation fires on diffuse radiation and forest productivity using a satellite-derived fire classification scheme [*van der Werf et al.,* 2010] to isolate deforestation fires from other types of landscape fires over the period 1998–2007. We estimate that deforestation fires result in increases of 15%, 1.7%, 0.4%, and 0.6% in PM2.5, diffuse radiation, GPP, and NPP, respectively (supporting information Figure S3), ~40% of the impact we calculated for all BBA.

The largest NPP increases are simulated in the southern part of the Amazon basin where NPP is enhanced up to 10% in the dry season (Figure 3). When integrating changes in NPP over 1997–2008, we calculate that forests in some southern Amazonia areas are accumulating an additional 400 kg C ha^{-1} a^{-1} (supporting information Figure S4). Amazon basin average NPP is increased by 128–258 kg C ha^{-1} a^{-1}, representing an increase of 78–156 Tg C a^{-1} when integrated across the basin. This compares with a decrease in terrestrial carbon storage of ~240 Tg C a^{-1} over the same period caused by direct emission of C by the fires [*van der Werf et al.,* 2010]. Thus, in terms of the terrestrial carbon budget, we estimate that the increase in productivity caused by impacts on diffuse radiation represents 33–65% of the direct emissions from biomass burning during 1998–2007. That is, remaining forests respond to changes in diffuse radiation by absorbing additional carbon and offsetting some of the original carbon emission from fires. However, it should be noted that this offset occurs only once, while the loss of forest caused by deforestation persists for decades. We also compared our calculated increase in NPP due to changes

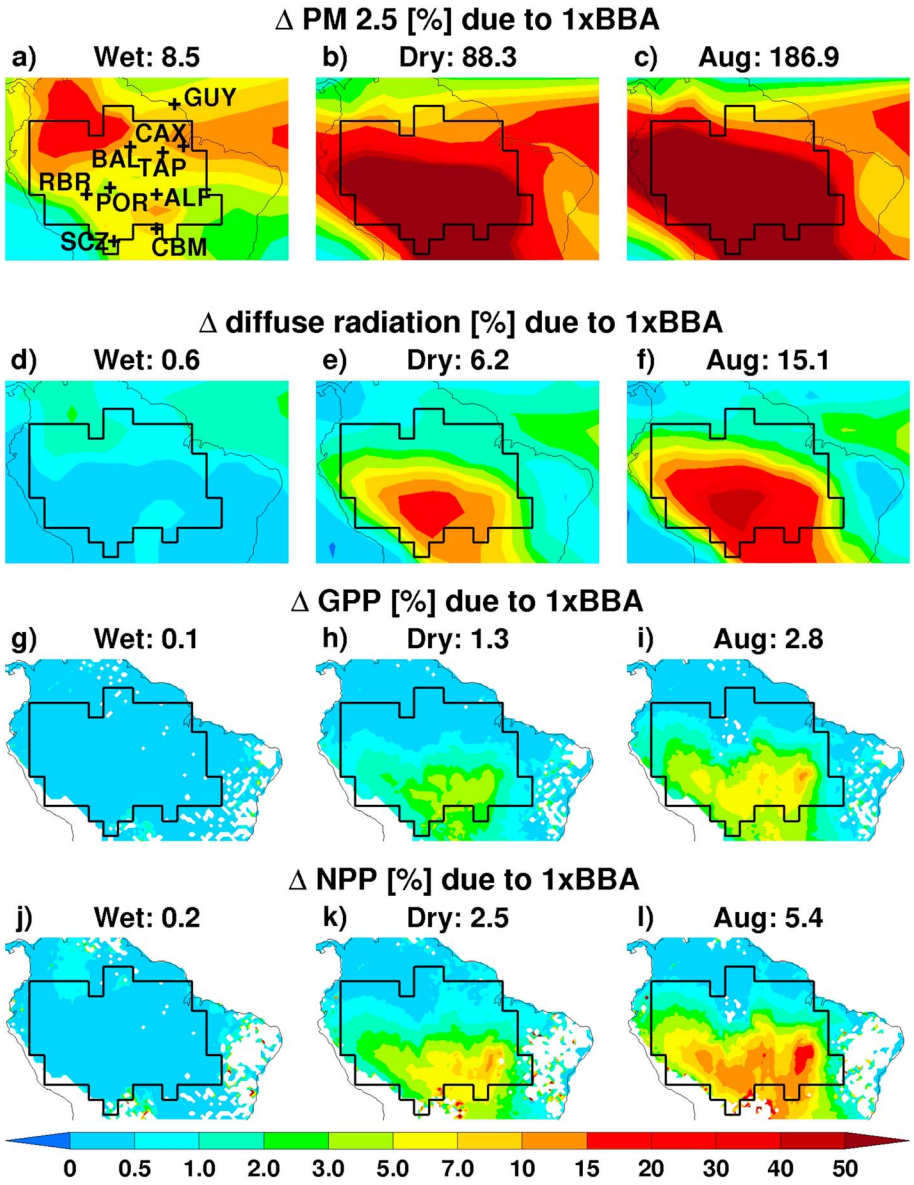

Figure 3. Modeled 1998–2007 mean percentage changes in (a–c) PM2.5, (d–f) diffuse radiation, (g–i) GPP, and (j–l) NPP during the wet (defined here as December to May) season (Figures 3a, 3d, 3g, and 3j), dry (June to November) season (Figures 3b, 3e, 3h, and 3k), and August (Figures 3c, 3f, 3i, and 3l) due to BBA emissions. Values above panels are Amazon basin (black line area boundary shown) averages. Figure 3a shows locations of the observation sites in Figures 1 and S1. (ALF: Alta Floresta; BAL: Balbina; CAX: Caxiuana; CBM: Cuiaba-Miranda; GUY: Guyaflux; POR: Porto Velho; RBR: Rio Branco; SCZ: Santa Cruz; TAP: Tapajos).

in diffuse radiation against the observed carbon sink [*Phillips et al.,* 2009]. Using a global data set of NPP allocation in tropical forests [*Malhi et al.,* 2011], we estimate that 30–60 Tg C a^{-1} of the simulated NPP increase corresponds to woody tissue, which represents 8–16% of the observed carbon sink across mature Amazonian forests [*Phillips et al.,* 2009].

Fires in Amazonia exhibit strong interannual variability driven by variability in climate [*Aragão et al.,* 2008], with the largest fractional changes in PM2.5 and diffuse radiation occurring during the dry seasons of 1998, 2005, and 2007, matching years with the largest fire emissions [*van der Werf et al.,* 2010] (supporting information Figure S5). We simulated greater NPP enhancement in these years with large fire emissions (Figure 4), though as a fraction of direct emissions of C by fires this enhancement decreased from 40–50% in low fire years to 25–30% in large fire years. During years with large fire activity, the reduction in total

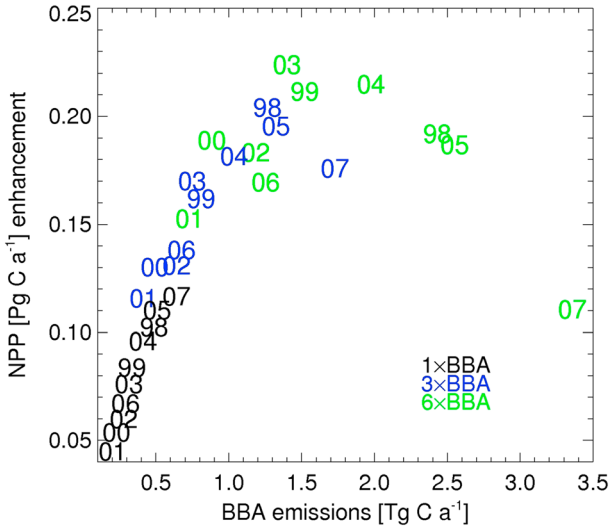

Figure 4. Amazon basin annual mean NPP enhancement caused by BBA as a function of BBA emissions (black: standard BBA emissions; blue: 3 × BBA emissions; and green: 6 × BBA emissions), for each year during 1998–2007.

radiation inhibits some of the diffuse radiation fertilization effect, reducing its efficacy. This is even more apparent in simulations where we increased the BBA emissions by a factor of 6: while in years with low fire activity (e.g., 2000 and 2001), this leads to further NPP enhancements, the effect is the opposite during years with large fire emissions (e.g., 1998, 2005, and 2007). The maximum increase in NPP occurs for an Amazon basin BBA emission of ~1.5 Tg C a^{-1} (Figure 4), with the negative environmental impacts of greater fire activity exacerbated further by a substantial reduction in the efficiency of the diffuse radiation fertilization effect.

The diffuse radiation fertilization effect of BBA occurs mainly during the dry season, when there is a simultaneous impact from moisture stress on GPP and NPP. A recent analysis of carbon flux measurements from Amazonian forest plots [*Gatti et al.,* 2014] shows that photosynthesis suppression during drought years has an important effect on the Amazonian carbon balance. This is also simulated in our model, where the Amazon basin NPP anomaly during the year 2005 (a drought year) compared to the 1998–2007 mean is −40 to −50 Tg C a^{-1}. A similar value of -50 ± 110 Tg C a^{-1} is calculated as the multimodel mean 2005 NPP anomaly from nine DGVMs [*Sitch et al.,* 2015] for the tropical South America region. However, in our simulation with no BBA impacts on radiation, the 2005 NPP anomaly is −80 Tg C a^{-1}, indicating that fertilization from diffuse radiation mitigates a substantial fraction (40–50%) of the moisture-generated decline in NPP in drought years. We therefore argue that the direct impact of moisture shortage on tropical production [*Gatti et al.,* 2014] may be larger than is observed, because in practice aerosols have tended to counteract its impacts through increased diffuse radiation.

We have accounted for uncertainty in BBA emissions; additional uncertainty is caused due to uncertainty in the composition of BBA and in aerosol optical properties. Increased aerosol absorption leads to reductions in downward irradiance without increasing diffuse radiation [*Jacobson*, 1999]. In this study we use the GLOMAP-mode aerosol optical properties from *Bellouin et al.* [2013] and simulate an Amazon basin dry season single-scattering albedo (SSA) at 0.55 μm of 0.94 ± 0.03 in our control simulation. Although toward the higher end, this is in relatively good agreement with existing Amazon SSA estimates such as 0.93 ± 0.03 from an AERONET site analysis [*Rosário et al.,* 2011], 0.92 ± 0.03 from MODIS retrievals [*Zhu et al.,* 2011], or 0.90–0.95 from lidar-derived estimates [*Baars et al.,* 2012]. To investigate the sensitivity of our results to BBA absorption properties, we performed additional simulations where we increased the BC fraction of BBA by factors of 2 and 4, which resulted in corresponding SSA values of 0.90 ± 0.05 and 0.85 ± 0.08, respectively (supporting information Figure S6). Increasing the BC fraction corresponds to an increase of BBA absorption properties, which alters the balance between the reduction in direct and the increase in diffuse radiation. The simulated increase in basin-wide annual mean NPP changes from 1.4% in the control simulation to 0.9% in the 2 × BC and 0.4% in the 4 × BC simulations, demonstrating sensitivity to optical properties of BBA, but with NPP enhancements even with more strongly absorbing aerosol. Our work demonstrates that the system is not just sensitive to the total emission of BBA but to the optical properties of the aerosol providing additional rationale for better constraining BBA single-scattering albedo.

The aim of this study was to isolate the impact of fires on vegetation through changes to diffuse radiation. Aerosol from fires may also increase CO_2 uptake by tropical forests through a reduction in leaf temperature. While this effect is minor for shaded leaves [*Doughty et al.,* 2010], this might not be the case for sunlit leaves,

implying that our estimated enhancement of NPP may be conservative. Biomass burning aerosol may also cause increased dry season length [*Bevan et al.,* 2009], alter patterns of precipitation [*Andreae et al.,* 2004; *Tosca et al.,* 2013], and change evapotranspiration, potentially causing further impacts on rainfall [*Spracklen et al.,* 2012]. Reductions in rainfall will reduce forest productivity, counteracting some of the changes that we simulate due to diffuse radiation. Fires also release a range of gas phase pollutants resulting in the production of ozone which can damage vegetation [*Pacifico et al.,* 2014]. Our coarse-resolution global model does not simulate the suppression of total radiation and photosynthesis under dense smoke plumes. A suggestion for further work beyond the scope of that presented here is repetition with higher-resolution models. Future studies also need to explore the impacts of fire in fully coupled Earth system models, although the complexity of these interactions, particularly aerosol-cloud interactions [*Rosenfeld et al.,* 2008], mean that uncertainties in the overall impact of BBA on the biosphere are likely to be large.

Acknowledgments

Data can bemade available upon request from the corresponding author. This research was funded by the Natural Environment Research Council (NE/J004723/1 and NE/J009822/1). P.A. was supported by FAPESP grants 2013/05014-0, 2014/50297-2 and CNPq. Data recorded in French Guiana benefited from an "Investissements d'Avenir" grant managed by Agence Nationale de la Recherche (CEBA ANR-10-LABX-25-01). We thank researchers from the TRENDY multimodel intercomparison project for access to data, the LBA central office at INPA for logistical support and the principal investigators and their staff for establishing and maintaining the AERONET sites used in this study.

The Editor thanks two anonymous reviewers for their assistance in evaluating this paper.

References

Andreae, M. O., D. Rosenfeld, P. Artaxo, A. A. Costa, G. P. Frank, K. M. Longo, and M. A. F. Silva-Dias (2004), Smoking rain clouds over the Amazon, *Science*, *303*(5662), 1337–1342.

Andreae, M. O., P. Artaxo, V. Beck, M. Bela, S. Freitas, C. Gerbig, K. Longo, J. W. Munger, K. T. Wiedemann, and S. C. Wofsy (2012), Carbon monoxide and related trace gases and aerosols over the Amazon Basin during the wet and dry seasons, *Atmos. Chem. Phys.*, *12*(13), 6041–6065.

Aragão, L. E. O. C., Y. Malhi, N. Barbier, A. Lima, Y. Shimabukuro, L. Anderson, and S. Saatchi (2008), Interactions between rainfall, deforestation and fires during recent years in the Brazilian Amazonia, *Philos. Trans. R. Soc. B*, *363*(1498), 1779–1785.

Artaxo, P., L. V. Rizzo, J. F. Brito, H. M. J. Barbosa, A. Arana, E. T. Sena, G. G. Cirino, W. Bastos, S. T. Martin, and M. O. Andreae (2013), Atmospheric aerosols in Amazonia and land use change: From natural biogenic to biomass burning conditions, *Faraday Discuss.*, *165*, 203–235.

Baars, H., A. Ansmann, D. Althausen, R. Engelmann, B. Heese, D. Müller, P. Artaxo, M. Paixao, T. Pauliquevis, and R. Souza (2012), Aerosol profiling with lidar in the Amazon Basin during the wet and dry season, *J. Geophys. Res.*, *117*, D21201, doi:10.1029/2012JD018338.

Bellouin, N., G. W. Mann, M. T. Woodhouse, C. Johnson, K. S. Carslaw, and M. Dalvi (2013), Impact of the modal aerosol scheme GLOMAP-mode on aerosol forcing in the Hadley Centre Global Environmental Model, *Atmos. Chem. Phys.*, *13*(6), 3027–3044.

Best, M. J., et al. (2011), The Joint UK Land Environment Simulator (JULES), model description—Part 1: Energy and water fluxes, *Geosci. Model Dev.*, *4*(3), 677–699.

Bevan, S. L., P. R. J. North, W. M. F. Grey, S. O. Los, and S. E. Plummer (2009), Impact of atmospheric aerosol from biomass burning on Amazon dry-season drought, *J. Geophys. Res.*, *114*, D09204, doi:10.1029/2008JD011112.

Bonal, D., et al. (2008), Impact of severe dry season on net ecosystem exchange in the Neotropical rainforest of French Guiana, *Global Change Biol.*, *14*(8), 1917–1933.

Butt, N., M. New, Y. Malhi, A. C. Lola da Costa, P. Oliveira, and J. E. Silva-Espejo (2010), Diffuse radiation and cloud fraction relationships in two contrasting Amazonian rainforest sites, *Agric. For. Meteorol.*, *150*(3), 361–368.

Clark, D. B., et al. (2011), The Joint UK Land Environment Simulator (JULES), model description—Part 2: Carbon fluxes and vegetation dynamics, *Geosci. Model Dev.*, *4*(3), 701–722.

Dai, Y. J., R. E. Dickinson, and Y. P. Wang (2004), A two-big-leaf model for canopy temperature, photosynthesis, and stomatal conductance, *J. Clim.*, *17*(12), 2281–2299.

Davidson, E. A., et al. (2012), The Amazon basin in transition, *Nature*, *481*(7381), 321–328.

Dentener, F., et al. (2006), Emissions of primary aerosol and precursor gases in the years 2000 and 1750 prescribed data-sets for AeroCom, *Atmos. Chem. Phys.*, *6*, 4321–4344.

Doughty, C. E., M. G. Flanner, and M. L. Goulden (2010), Effect of smoke on subcanopy shaded light, canopy temperature, and carbon dioxide uptake in an Amazon rainforest, *Global Biogeochem. Cycles*, *24*, GB3015, doi:10.1029/2009GB003670.

Edwards, J. M., and A. Slingo (1996), Studies with a flexible new radiation code. 1: Choosing a configuration for a large-scale model, *Q. J. R. Meteorol. Soc.*, *122*(531), 689–719.

Gatti, L. V., et al. (2014), Drought sensitivity of Amazonian carbon balance revealed by atmospheric measurements, *Nature*, *506*(7486), 76–80.

Gu, L. H., D. D. Baldocchi, S. C. Wofsy, J. W. Munger, J. J. Michalsky, S. P. Urbanski, and T. A. Boden (2003), Response of a deciduous forest to the Mount Pinatubo eruption: Enhanced photosynthesis, *Science*, *299*(5615), 2035–2038.

Hoelzemann, J. J., K. M. Longo, R. M. Fonseca, N. M. E. do Rosário, H. Elbern, S. R. Freitas, and C. Pires (2009), Regional representativity of AERONET observation sites during the biomass burning season in South America determined by correlation studies with MODIS aerosol optical depth, *J. Geophys. Res.*, *114*, D13301, doi:10.1029/2008JD010369.

Holben, B. N., et al. (2001), An emerging ground-based aerosol climatology: Aerosol optical depth from AERONET, *J. Geophys. Res.*, *106*(D11), 12,067–12,097, doi:10.1029/2001JD900014.

Harmonized World Soil Database (2012), *HWSD/FAO/IIASA/ISRIC/ISSCAS/JRC, Harmonized World Soil Database (Version 1.2)*, FAO, Rome and IIASA, Laxenburg, Austria.

Jacobson, M. Z. (1999), Isolating nitrated and aromatic aerosols and nitrated aromatic gases as sources of ultraviolet light absorption, *J. Geophys. Res.*, *104*(D3), 3527–3542, doi:10.1029/1998JD100054.

Kaiser, J. W., et al. (2012), Biomass burning emissions estimated with a global fire assimilation system based on observed fire radiative power, *Biogeosciences*, *9*(1), 527–554.

Lewis, S. L., Y. Malhi, and O. L. Phillips (2004), Fingerprinting the impacts of global change on tropical forests, *Philos. Trans. R. Soc. London, Ser. B*, *359*(1443), 437–462.

Malhi, Y., C. Doughty, and D. Galbraith (2011), The allocation of ecosystem net primary productivity in tropical forests, *Philos. Trans. R. Soc. B*, *366*(1582), 3225–3245.

Mann, G. W., K. S. Carslaw, D. V. Spracklen, D. A. Ridley, P. T. Manktelow, M. P. Chipperfield, S. J. Pickering, and C. E. Johnson (2010), Description and evaluation of GLOMAP-mode: A modal global aerosol microphysics model for the UKCA composition-climate model, *Geosci. Model Dev.*, *3*(2), 519–551.

Martin, S. T., et al. (2010), Sources and properties of Amazonian aerosol particles, *Rev. Geophys.*, *48*, RG2002, doi:10.1029/2008RG000280.

Mercado, L. M., C. Huntingford, J. H. C. Gash, P. M. Cox, and V. Jogireddy (2007), Improving the representation of radiation interception and photosynthesis for climate model applications, *Tellus, Ser. B*, *59*(3), 553–565.
Mercado, L. M., N. Bellouin, S. Sitch, O. Boucher, C. Huntingford, M. Wild, and P. M. Cox (2009), Impact of changes in diffuse radiation on the global land carbon sink, *Nature*, *458*(7241), 1014–1017.
Nemani, R. R., C. D. Keeling, H. Hashimoto, W. M. Jolly, S. C. Piper, C. J. Tucker, R. B. Myneni, and S. W. Running (2003), Climate-driven increases in global terrestrial net primary production from 1982 to 1999, *Science*, *300*(5625), 1560–1563.
Niyogi, D., et al. (2004), Direct observations of the effects of aerosol loading on net ecosystem CO_2 exchanges over different landscapes, *Geophys. Res. Lett.*, *31*, L20506, doi:10.1029/2004GL020915.
Oliveira, P. H. F., P. Artaxo, C. Pires, S. De Lucca, A. Procopio, B. Holben, J. Schafer, L. F. Cardoso, S. C. Wofsy, and H. R. Rocha (2007), The effects of biomass burning aerosols and clouds on the CO_2 flux in Amazonia, *Tellus, Ser. B*, *59*(3), 338–349.
Pacifico, F., G. A. Folberth, S. Sitch, J. M. Haywood, P. Artaxo, and L. V. Rizzo (2014), Biomass burning related ozone damage on vegetation over the Amazon forest, *Atmos. Chem. Phys. Discuss.*, *14*(14), 19,955–19,983.
Phillips, O. L., et al. (2009), Drought sensitivity of the Amazon rainforest, *Science*, *323*(5919), 1344–1347.
Rap, A., C. E. Scott, D. V. Spracklen, N. Bellouin, P. M. Forster, K. S. Carslaw, A. Schmidt, and G. Mann (2013), Natural aerosol direct and indirect radiative effects, *Geophys. Res. Lett.*, *40*, 3297–3301, doi:10.1002/grl.50441.
Restrepo-Coupe, N., et al. (2013), What drives the seasonality of photosynthesis across the Amazon basin? A cross-site analysis of eddy flux tower measurements from the Brasil flux network, *Agric. For. Meteorol.*, *182–183*, 128–144.
Roderick, M. L., G. D. Farquhar, S. L. Berry, and I. R. Noble (2001), On the direct effect of clouds and atmospheric particles on the productivity and structure of vegetation, *Oecologia*, *129*(1), 21–30.
Rosário, N. E., M. A. Yamasoe, H. Brindley, T. F. Eck, and J. Schafer (2011), Downwelling solar irradiance in the biomass burning region of the southern Amazon: Dependence on aerosol intensive optical properties and role of water vapor, *J. Geophys. Res.*, *116*, D18304, doi:10.1029/2011JD015956.
Rosenfeld, D., U. Lohmann, G. B. Raga, C. D. O'Dowd, M. Kulmala, S. Fuzzi, A. Reissell, and M. O. Andreae (2008), Flood or drought: How do aerosols affect precipitation?, *Science*, *321*(5894), 1309–1313.
Rossow, W. B., and R. A. Schiffer (1999), Advances in understanding clouds from ISCCP, *Bull. Am. Meteorol. Soc.*, *80*(11), 2261–2287.
Saleska, S. R., et al. (2003), Carbon in Amazon forests: Unexpected seasonal fluxes and disturbance-induced losses, *Science*, *302*(5650), 1554–1557.
Schafer, J. S., B. N. Holben, T. F. Eck, M. A. Yamasoe, and P. Artaxo (2002), Atmospheric effects on insolation in the Brazilian Amazon: Observed modification of solar radiation by clouds and smoke and derived single scattering albedo of fire aerosols, *J. Geophys. Res.*, *107*(D20), 8074, doi:10.1029/2001JD000428.
Sellers, P. J. (1985), Canopy reflectance, photosynthesis and transpiration, *Int. J. Remote Sens.*, *6*(8), 1335–1372.
Sitch, S., et al. (2015), Recent trends and drivers of regional sources and sinks of carbon dioxide, *Biogeosciences*, *12*(3), 653–679.
Spracklen, D. V., S. R. Arnold, and C. M. Taylor (2012), Observations of increased tropical rainfall preceded by air passage over forests, *Nature*, *489*(7415), 282–285.
Tosca, M. G., J. T. Randerson, and C. S. Zender (2013), Global impact of smoke aerosols from landscape fires on climate and the Hadley circulation, *Atmos. Chem. Phys.*, *13*(10), 5227–5241.
van der Werf, G. R., J. T. Randerson, L. Giglio, G. J. Collatz, M. Mu, P. S. Kasibhatla, D. C. Morton, R. S. DeFries, Y. Jin, and T. T. van Leeuwen (2010), Global fire emissions and the contribution of deforestation, savanna, forest, agricultural, and peat fires (1997–2009), *Atmos. Chem. Phys.*, *10*(23), 11,707–11,735.
van Genuchten, M. T. (1980), A closed-form equation for predicting the hydraulic conductivity of unsaturated soils, *Soil Sci. Soc. Am. J.*, *44*(5), 892–898.
Weedon, G. P., S. Gomes, P. Viterbo, W. J. Shuttleworth, E. Blyth, H. Oesterle, J. C. Adam, N. Bellouin, O. Boucher, and M. Best (2011), Creation of the WATCH forcing data and its use to assess global and regional reference crop evaporation over land during the twentieth century, *J. Hydrometeorol.*, *12*(5), 823–848.
Wood, J., T. Muneer, and J. Kubie (2003), Evaluation of a new photodiode sensor for measuring global and diffuse irradiance, and sunshine duration, *J. Sol. Energy Eng.*, *125*(1), 43–48.
Zhu, L., J. V. Martins, and L. A. Remer (2011), Biomass burning aerosol absorption measurements with MODIS using the critical reflectance method, *J. Geophys. Res.*, *116*, D07202, doi:10.1029/2010JD015187.